Optimal Cooperation Strategy in Cognitive Radio Systems with Energy Harvesting

Sixing Yin, *Member, IEEE*, Erqing Zhang, Zhaowei Qu, Liang Yin, and Shufang Li, *Senior Member, IEEE*

***Abstract*—In recent years, the excessive energy consumption in wireless communication systems has been increasingly critical, and environmental and financial considerations have motivated a trend in wireless communication technologies to resort to renewable energy sources. Energy harvesting is considered as a promising solution to alleviate such issues and has received extensive attentions. In this paper, we consider a cognitive radio system with one primary user (PU) and one secondary user (SU) and both of their transmitters operate in time-slotted mode. The SU, which harvests energy exclusively from ambient radio signal, follows a *save-then-transmit* protocol. In such a scenario, we investigate the SU's optimal cooperation strategy, namely, the optimal decision (to cooperate with the PU or not) and the optimal action (to spend how much time on energy harvesting and to allocate how much power for cooperative relay). We separately investigate the optimal action in non-cooperation and cooperation modes to maximize the SU's achievable throughout and derive the optimal closed-form solutions. Based on the analytical results of the optimal solutions, we propose the optimal cooperation protocol (OCP) to make the optimal decision, which simply involves a two-level test. Simulation results show that the proposed OCP outperforms the other two protocols (non-cooperation protocol and stochastic cooperation protocol) and the optimal underlay (OU) transmission mode.**

***Index Terms*—Cognitive radio, cooperative communication, energy harvesting.**

I. Introduction

In recent years, with the rapid growth in wireless communication applications, the increasing rigidity of environmental standards as well as the tremendous rise in energy cost, issues in energy consumption has become increasingly critical, which calls for solutions for improving the energy efficiency of wireless communication technologies [1].

In addition to energy-efficient wireless communication technologies, energy harvesting communication systems powered either largely or exclusively by renewable sources are considered as another helpful option that can significantly alleviate energy-deficiency and have become increasingly attractive [2]. Unlike conventional battery-powered communication systems, energy harvesting could potentially provide unlimited energy supply from the environment in a much easier and safer way for conventional energy-constrained wireless communication systems, such as wireless sensor networks (WSNs).

As one of the emerging wireless technologies, cognitive radio (CR) is considered as a promising solution for improving spectrum efficiency by allowing secondary users (SUs) opportunistically to utilize the spectrum unused by primary (licensed) users (PUs). However, exclusive functionalities such as spectrum sensing potentially make CR devices more energy-consuming. In this sense, issues in energy efficiency could be even more severe in CR systems than in conventional wireless communication systems such that energy-efficient spectrum sharing has received much attention.

Cooperative communication has also been a hot topic in wireless networks and extensively studied in terms of either spatial reusability enhancement (e.g., multi-hop *ad hoc* networks) or coverage range expansion (e.g., cellular networks). Cooperation between PUs and SUs in CR networks can be also helpful in terms of more secondary transmission opportunities [3]. In CR systems, instead of keeping silent when PUs are busy, SUs can alternatively act as cooperative relays to improve the PUs' throughput, which could lead to earlier completion of the PUs' transmission and further more opportunities for secondary transmission. By this means, even in case that PUs monopolize the licensed channels all the time, SUs can still squeeze out transmission opportunities rather than suffer from the helpless "starvation".

In this paper, we consider a CR system with one pair of primary transceiver and one pair of secondary transceiver, which operate in time-slotted mode. The SU transmitter is powered exclusively by energy extracted from ambient radio signal. In order for data transmission on vacant licensed channels, the SU can either wait until the PU finishes its transmission or cooperates with the PU to make that happen earlier. In such a scenario, there exist non-trivial tradeoffs between the SU's energy harvesting (e.g., fraction of dedicated time), cooperative transmission (e.g., allocated power for cooperative relay) and data transmission. To tackle such tradeoffs, we investigate the optimal cooperation strategy in an energy harvesting CR system, namely, the optimal decision (to cooperate with the PU or not) and the optimal action (to spend how much time on energy harvesting and to allocate how much power for cooperative relay).

To the best of our knowledge, this work is the first to explore the cooperation strategies in the context of CR systems with energy harvesting to improve the SU's achievable throughput,

Manuscript received December 16, 2012; revised May 5, 2013, August 28, 2013, and November 19, 2013; accepted January 14, 2014. Date of publication July 1, 2014; date of current version September 8, 2014. The work was supported in part by the National Natural Science Foundation of China under Grant 61372109, the National Science and Technology Major Project under Grant 2012ZX03003006 and the Fundamental Research Funds for the Central Universities under Grant 2013RC0117. The associate editor coordinating the review of this paper and approving it for publication was M. Bhatnagar.

The authors are with Beijing University of Posts and Telecommunications, Beijing 100876, China (e-mail: yinsixing@bupt.edu.cn; zhangerqing@bupt.edu.cn; zwqu@bupt.edu.cn; yinl@bupt.edu.cn; lisf@bupt.edu.cn).

Color versions of one or more of the figures in this paper are available online at http://ieeexplore.ieee.org.

Digital Object Identifier 10.1109/TWC.2014.2322972

as well as to present a practical protocol design. The main contributions of this paper are summarized as follows:

1) By proving the concavity of the achievable throughput maximization problem in non-cooperation mode, we derive the closed-form solution (the optimal save-ratio) in non-cooperation mode and numerically analyze the impact of various system parameters.
2) With in-depth analysis on the convexity and optimality conditions of the achievable throughput maximization problem in cooperation mode, we derive the closed-form solution (the optimal save-ratio and allocated power for cooperative relay) in cooperation mode following decode-and-forward (DF) protocol and numerically analyze the impact of various system parameters.
3) Based on the analytical results in both non-cooperation and cooperation modes, we further investigate the SU's optimal decision (to cooperate with the PU or not) and propose the optimal cooperation protocol, which compares the optimal achievable throughput in the two modes through a simple two-level test, and evaluate its performance compared with the other two protocols (non-cooperation protocol and stochastic cooperation protocol) and the optimal underlay transmission mode.

The remainder of this paper is organized as follows. Related works are introduced in Section II. In Section III, we describe the system model of both non-cooperation and cooperation modes. In Section IV, we formulate the achievable throughput maximization problem in non-cooperation and cooperation modes, respectively. Then in Section V, we separately derive the optimal closed-form solutions in non-cooperation and cooperation modes, which are further numerically analyzed with impact of various system parameters in Section VI. Based on the analytical results, the proposed optimal cooperation protocol is elaborated in Section VII and its performance is evaluated through simulations in Section VIII. Key points in implementing the optimal cooperation protocol are discussed and corresponding proposals are made in Section IX. Finally, we conclude this paper in Section X.

II. Related Works

A. Cooperation Mechanism in CR Systems

Cognitive radio was proposed to improve the spectrum utilization by allowing SUs to opportunistically exploit the spectrum unused by PUs. Meanwhile, cooperation mechanism has been considered as a key technology for increasing transmission diversity gain in CR systems.

Cooperative interaction between PUs and SUs has been extensively studied in recent years. In [4], a scenario in which the SU acts as a relay for the packets it successfully receives from the primary source but are not received by the primary destination is considered and the stable throughput of the SU under this model is derived. The authors in [5] propose the "cooperative cognitive radio networks" in which PUs lease a portion of the licensed spectrum to SUs in return for cooperative relaying and model the spectrum leasing strategies as a Stackelberg game. Similar scenario and model take place in [6], where a primary link has the possibility to lease the owned spectrum to an *ad hoc* network of secondary nodes in exchange for cooperation in the form of distributed space-time coding. In [7], the authors consider cooperation between PUs and SUs and investigate multi-access protocols allowing simultaneous transmission of relaying and secondary databased on dirty-paper coding (DPC), which introduces a tradeoff between PU and SU performance combining with opportunistic relay selection. In [8], an overlay spectrum sharing scheme where the PU leases half of its timeslots to the SU in exchange for the SU's cooperatively relaying the PU's data is investigated and the SU's antenna weights design and power allocation scheme are proposed to meet a certain error or rate design criterion for both PU and SU. In [9], opportunistic cooperation between secondary (femtocell) users and primary (macrocell) users in cognitive femtocell networks is investigated and SU's throughput-optimal cooperation decisions are derived with a greedy and online control algorithm using a generalized Lyapunov optimization technique.

There are also a large number of literatures on cooperative spectrum sensing due to its advantages over individual spectrum sensing in terms of immunity to fading and shadowing channels. In [10], the authors investigate optimization for the cooperative spectrum sensing with an improved energy detector to minimize the total error rate (sum of the probability of false alarm and miss detection). Follow-up works extend the scenario in [10] to imperfect reporting channels [11] and SUs with multiple antennas [12], respectively. Cooperative spectrum sensing based on finite number of primary signal samples is investigated in [13] and [14], where the local and global thresholds are optimized in order to minimize the total error rate.

B. Energy Harvesting in Communication Systems

As a hot topic that attracts tremendous interests, analysis of energy harvesting communication systems powered by renewable sources has been first performed from the perspective of information theory in [15] and [16], based on which throughput optimization for energy harvesting communications has been extensively studied. In [17] and [18], throughput optimization for an energy harvesting transmitter with a deadline constraint is studied under static channel condition. In [19]–[21] (the followup work of [18]), throughput optimization problems are extended to fading and multi-access channels. In addition to other commonly used energy sources (e.g., solar and wind), ambient radio signal is considered as another viable energy source since it carries energy as well as information at the same time. Consequently, simultaneous wireless information and power transfer becomes appealing since it takes advantages of interference signal which used to be eliminated in conventional wireless networks. Simultaneous information and power transfer over the wireless channels has been initially studied in [22] and [23]. In [22], the authors first propose the idea of transmitting information and energy simultaneously as well as a capacity-energy function to characterize the fundamental tradeoffs. In [23], the authors extend the work in [22] to frequency-selective channels with AWGN and show that a non-trivial tradeoff exists

in frequency-domain power allocation for maximal information versus energy transfer. There have been several other existing works on simultaneous information and power transfer. In [24], a "save-then-transmit protocol" is proposed to optimize the system outage performance with the optimal save-ratio. In [25], the authors derive the optimal switching rule between the information decoding mode and the energy harvesting mode to minimize the outage probability. Moreover, in [26] and [27], the rate-energy region characterization is extended to MIMO systems.

C. Energy Harvesting in CR Systems

There have been also several prior works that consider CR systems powered by energy harvesting [28]–[30]. [28] formulates the optimal sensing and access policies as a Markov decision process and derives the optimal policy by the probability of PU's presence and the amount of stored energy. [29] considers a cognitive radio sensor network powered by RF energy harvesting and formulates the optimal mode selection ("access" or "harvest") policy as a partially observable Markov decision process (POMDP). In [31], spatial spectrum reuse in CR networks with energy harvesting is investigated based on a stochastic-geometry model where the primary and secondary transmitters are modeled as independent homogeneous Poisson point processes (HPPPs). In [30], the authors provide an optimal spectrum sensing policy for an energy-harvesting CR that maximizes the expected total throughput under energy causality and collision constraints. Compared with these works, the salient feature of this paper is that, by considering the aforementioned tradeoffs between energy harvesting, cooperative communication and secondary transmission, we investigate the optimal cooperation strategy that maximizes the SU's achievable throughput and further present a practical protocol design based on the optimal closed-form solutions.

III. System Model

We consider a CR system with one pair of primary transceiver and one pair of secondary transceiver and both of them operate in time-slotted mode shown in Fig. 1.

The PU has the ownership of a licensed channel and transmits to its receiver whenever it has data to send. The PU has a certain amount of data stored in its buffer. In each timeslot, the PU uses the licensed channel to transmit its data. After all of PU's data is transmitted, the PU turns to silence and the licensed channel is vacated. In contrast, the SU does not have any licensed spectrum and is allowed to transmit its own data only when the licensed channel is unused by the PU in order to avoid collision with the PU. Moreover, the self-powered SU has no fixed power supplies and extracts energy exclusively via energy harvested from ambient radio signal. We also assume that the SU's transmitter follows a *save-then-transmit* protocol. This is because practically rechargeable energy storage devices cannot charge and discharge simultaneously (which is termed energy half-duplex constraint [24]). In each timeslot, the SU first devotes a fraction (referred to as save-ratio) of time exclusively to energy harvesting, then it uses the harvested energy for data transmission.

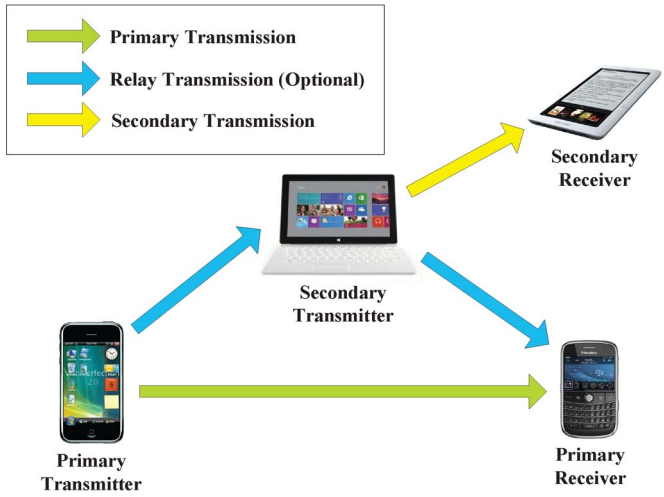

Fig. 1. CR systems with cooperation between PU and SU.

In such a CR system, the SU cannot transmit its data when the licensed channel is being used by the PU. It can transmit its data only during the period when PU is absent on the licensed channel to prevent the interference incurred at the primary receiver by secondary transmission. However, instead of keeping silent when the PU is busy, the SU can alternatively act as a cooperative relay to improve the PU's throughput, which results in earlier completion of the PU's transmission and further opportunities for secondary transmission. By this means, even in case that the PU monopolizes the licensed channel all the time, opportunities for secondary transmission can still be squeezed out. Therefore, cooperative communication between PU and SU is considered as the SU's option to potentially increase the PU's throughput such that the licensed channel could be vacated and more transmission opportunities could be provided for the SU.[1]

In order to do so, the SU must consume its harvested energy to help relay the PU's data. This cooperation can take place in several ways depending on the cooperative protocol being used. In this paper, we assume the cooperative communication between PU and SU follows the decode-and-forward (DF) protocol, which is one of the commonly used protocols. In the DF protocol, the relays first decode the received signal, re-encode it, and then transmit it to the destination. Finally, the destination uses both the signals jointly to decode the data. More details of the DF protocol are presented in Section III-B.

The notations used in this paper are summarized in Table I. Here, we have

$$R_p = \log_2(1+\gamma_p) \tag{1}$$

for PU's instantaneous non-cooperative transmission rate. In the following part of this section, we elaborate the timeslot structure for both non-cooperation and cooperation modes.

[1]Cooperation from the SU causes neither benefit nor loss to the PU since it has a fixed amount of data to transmit within one timeslot and the motivation of PUs to accept cooperation from the SU is out of the scope of this paper.

TABLE I
NOTATIONS

T	Timeslot duration
Q	PU's data amount to send in each timeslot
X	SU's energy harvesting rate
R_p	PU's instantaneous non-cooperative transmission rate
R_c	PU's instantaneous cooperative transmission rate
t_c	Cooperative communication duration
r_s	Channel-power-gain-to-noise-power ratio of link between SU transceiver pair
r_p	Channel-power-gain-to-noise-power ratio of link between SU transmitter (relay) and PU receiver (destination)
γ_p	Signal-to-noise ratio of direct primary link at PU receiver
γ_s	Signal-to-noise ratio of link between PU transmitter (source) and SU transmitter (relay)
ρ	SU's save-ratio (to be optimized)
w	SU's allocated power for cooperative relay (to be optimized)

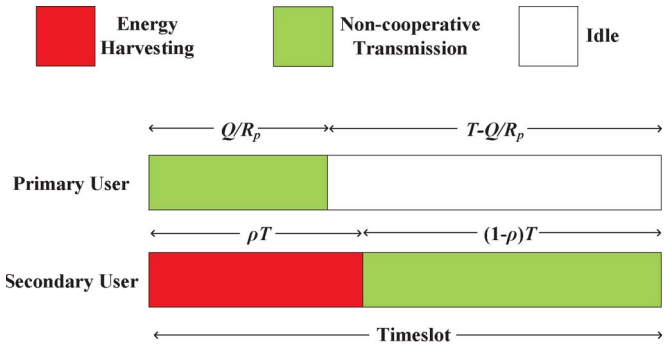

Fig. 2. Timeslot structure of non-cooperation mode in CR systems. The SU first collects energy from ambient radio signal and is allowed to transmit its own data only when the PU's transmission is finished.

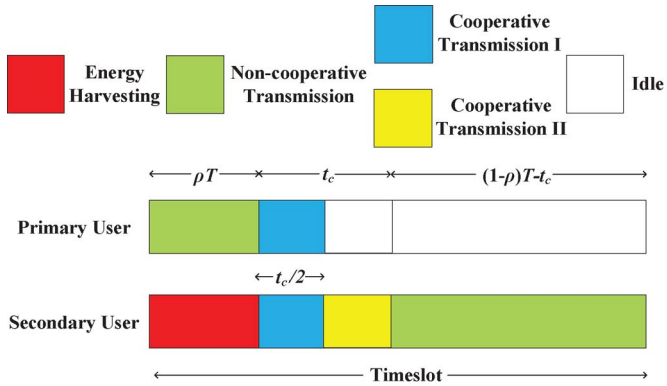

Fig. 3. Timeslot structure of cooperation mode in CR systems. During "Cooperative Transmission I", the PU transmitter transmits its data to the SU transmitter and PU receiver. During "Cooperative Transmission II", the SU transmitter relays the PU's data to the PU receiver.

A. Non-Cooperation Mode

In non-cooperation mode as shown in Fig. 2, the PU uses the licensed channel to transmit its data either without cooperation from the SU during time interval $(0, Q/R_p]$ and stay idle after finishing its transmission during time interval $(Q/R_p, T]$. Accordingly, during time interval $(0, \rho T]$, the SU collects energy from ambient radio signal and deposits the energy into a storage device while its transmitter is powered off since it cannot use the licensed channel unless the PU completes transmission. Thus, we have $\rho \geq Q/R_pT$ in non-cooperation mode. Then during time interval $(\rho T, T]$, the SU's energy harvester stops working and its transmitter is powered on for data transmission with energy in the storage device. Since in this paper, we focus on "myopic" (rather than long-term) optimization for the SU's achievable throughput in each timeslot, we assume that the SU must exhaust all the harvested energy in each timeslot for data transmission because it is meaningless to "penny-pinch" the harvested energy, which means that the SU's energy storage is emptied at the beginning of each timeslot.

The SU's activities (relaying or transmitting) are powered exclusively by energy harvested from ambient signal. Following the save-then-transmit protocol, the SU devotes a fraction of time to energy harvesting in each timeslot as shown in Fig. 2. In time-slotted operation mode, with more time spent on energy harvesting (higher save-ratio), more energy can be harvested, which leads to higher SU's instantaneous transmission rate, whereas less time remains for secondary transmission, which downgrades the SU's achievable throughput.

B. Cooperation Mode

In cooperation mode shown in Fig. 3, a timeslot is partitioned into three fractions synchronous for both PU and SU, which can be detailed as follows:

1) During time interval $(0, \rho T]$, the SU harvests energy from ambient signal while the PU transmits its data non-cooperatively. The SU's harvested energy amounts to $X\rho T$, where X denotes the SU's energy harvesting rate (average energy harvested in unit time). Meanwhile, the PU completes transmitting $R_p\rho T$ of data without cooperation and $Q - R_p\rho T$ of data is still left in the PU's buffer to send.
2) During time interval $(\rho T, \rho T + t_c]$, where the cooperative communication duration t_c is given by

$$t_c = \frac{Q - R_p\rho T}{R_c} \tag{2}$$

the PU and SU cooperate with each other helping improve the PU's throughput to complete the PU's transmission earlier. Here, we specify that $t_c \geq 0$ (namely, $\rho \leq Q/R_pT$) and that $R_pT \geq Q$ because the PU must be able to complete its transmission within one timeslot even without the SU's cooperation. Specially, the CR system turns non-cooperative for the case $t_c = 0$. Therefore, ρ is bounded within $[0, Q/R_pT]$. After consuming wt_c of energy for cooperative relay, $X\rho T - wt_c$ of energy remains. Following the DF protocol, which operates in

a time-division approach due to the half-duplex limitation in most of current radio implementations [32], the PU transmitter (as source) transmits its data to the SU transmitter (as relay) and PU receiver (as destination) in the first half of cooperation interval $(\rho T, \rho T + (t_c/2)]$. Then in the second half of cooperation interval $(\rho T + (t_c/2), \rho T + t_c]$, the SU transmitter relays the PU's data to the PU receiver. Here, we focus on fully decoding at the SU's transmitter (i.e., repetition-coded scheme without error). Therefore, we have

$$R_c = \frac{1}{2}\min\left\{\log_2(1+\gamma_s), \log_2(1+\gamma_p + w r_p)\right\} \quad (3)$$

for PU's instantaneous cooperative transmission rate following the DF protocol [32], [33]. Here, the first term in (3) represents the maximum rate at which the relay can reliably decode the source message, while the second term represents the maximum rate at which the destination can reliably decode the source message given repeated transmissions from the source and destination.

3) During time interval $(\rho T + t_c, T]$, when PU's transmission is completed and the licensed channel is vacated, the SU starts to transmit its own data. The PU keeps silent and $X\rho T - w t_c$ of energy remains for secondary transmission. Similar with non-cooperation mode, we assume that the SU must exhaust all the harvested energy in each timeslot for data transmission.

While operating in cooperation mode, in addition to the save-ratio, SU can decide how much of its harvested energy is allocated to help relay the PU's data as well. Evidently, with more energy consumed for cooperative relay, PU's transmission could be completed earlier such that more opportunities could be available for secondary transmission, whereas less energy is reserved, which inevitably limits the SU's achievable throughput.

IV. Problem Formulation

In this section, problems of the SU's achievable throughput maximization in non-cooperation and cooperation modes are formulated separately.

A. Non-Cooperation Mode

In non-cooperation mode as shown in Fig. 2, the SU's achievable throughput in each timeslot is given by

$$R_0(\rho) = (1-\rho)\log_2\left(1 + \frac{X\rho r_s}{1-\rho}\right) \quad (4)$$

and we aim at selecting the optimal save-ratio (ρ) to maximize the SU's achievable throughput and the problem can be formulated as the following:

$$\begin{aligned} \max_{\rho} \quad & R_0(\rho) \\ \text{s.t.} \quad & \frac{Q}{R_p T} \le \rho \le 1 \end{aligned} \quad (5)$$

The constraint in (5) guarantees that the SU should not initiate its transmission until the PU's transmission is completed. Note that $0 \le \rho < Q/R_p T$ seems also feasible, however, in non-cooperation mode, the SU has to wait in vain for the completion of PU's transmission in that case, which leads to loss of harvested energy and further non-optimal achievable throughput. Thus, we bound save-ratio within range $[Q/R_p T, 1]$ in non-cooperation mode.

B. Cooperation Mode

In cooperation mode as shown in Fig. 3, the SU's achievable throughput in each timeslot is given by

$$R_1(\rho, w) = ((1-\rho)T - t_c)\log_2\left(1 + \frac{(X\rho T - w t_c) r_s}{(1-\rho)T - t_c}\right) \quad (6)$$

Note that the SU's achievable throughput in (6) is normalized with $1/T$. We aim at jointly optimizing the SU's save-ratio (ρ) and allocated power for cooperative relay (w) to maximize SU's achievable throughput and the problem can be formulated as the following:

$$\begin{aligned} \max_{\rho, w} \quad & R_1(\rho, w) \\ \text{s.t.} \quad & (1-\rho)T - t_c \ge 0 \\ & X\rho T - w t_c \ge 0 \\ & 0 \le \rho \le \frac{Q}{R_p T} \\ & w \ge 0. \end{aligned} \quad (7)$$

The first constraint in (7) refers to the time causality constraint which guarantees that the cooperative communication duration should not exceed the remaining time after energy harvesting while the second one refers to the energy causality constraint which guarantees that the energy consumed for cooperative relay should not exceed the SU's harvested energy.

V. Achievable Throughput Maximization

In this section, we maximize the SU's achievable throughput in non-cooperation and cooperation modes, respectively.

A. Non-Cooperation Mode

In non-cooperation mode, we aim at selecting optimal save-ratio (ρ) to maximize the SU's achievable throughput in (5).

Lemma 1: $R_0(\rho)$ is concave while $0 \le \rho \le 1$.

Proof: Please refer to Appendix A. ■

Theorem 1: $R_0(\rho)$ attains the global optimality at

$$\rho_{nc} = \frac{X r_s - 1 - W\left(\frac{X r_s - 1}{\mathrm{e}}\right)}{(X r_s - 1)\left(W\left(\frac{X r_s - 1}{\mathrm{e}}\right) + 1\right)} \quad (8)$$

for $0 \le \rho \le 1$, where $W(.)$ refers to the Lambert W function [34].

Proof: Please refer to Appendix B. ■

Since ρ is bounded within $[Q/R_p T, 1]$, in which $R_0(\rho)$ is concave according to Lemma 1, the SU's optimal save-ratio in non-cooperation mode can be derived as

$$\rho_{nc}^* = \max\left\{\rho_{nc}, \frac{Q}{R_p T}\right\} \quad (9)$$

which is graphically interpreted by Fig. 4 (where the red dot represents the optimal save-ratio).

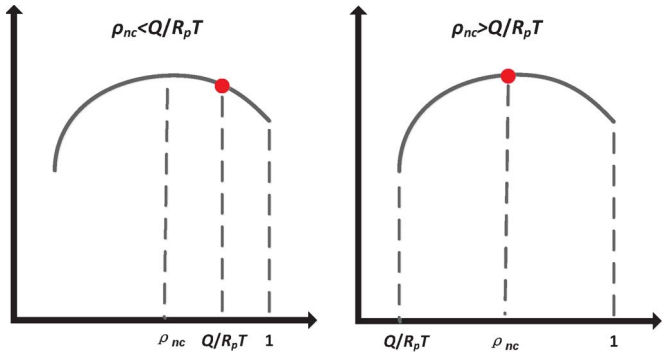

Fig. 4. Graphical interpretation for the optimal save-ratio in non-cooperation mode.

B. Cooperation Mode

In cooperation mode, we aim at jointly optimizing the SU's save-ratio (ρ) and allocated power for cooperative relay (w) to maximize SU's achievable throughput in (7). We first investigate the convexity of the optimization problem in (7) and then derive the optimal ρ and w by solving the equation system of Karush-Kuhn-Tucker (KKT) optimality conditions [35].

Lemma 2: The function $f(A,B) = A\ln(1+(B/A))$ is monotonically increasing for $A, B > 0$.

Proof: Please refer to Appendix C. ■

Theorem 2: The optimization problem in (7) is convex over ρ and w for $0 \le \rho \le Q/R_pT$ and $w \ge (\gamma_s - \gamma_p)/r_p$, while quasi-convex over w for $0 \le w < (\gamma_s - \gamma_p)/r_p$.

Proof: Please refer to Appendix D. ■

While $w \ge (\gamma_s - \gamma_p)/r_p$, t_c is independent of w and $t_c \ge 0$, $R_1(\rho, w)$ is non-increasing in w for any $0 \le \rho \le Q/R_pT$. Therefore, $R_1(\rho, w)$ attains its optimum at $w = (\gamma_s - \gamma_p)/r_p$. Moreover, according to (3), PU's instantaneous cooperative transmission rate can be rewritten as

$$R_c = \begin{cases} \frac{1}{2}\log_2(1+\gamma_p + wr_p), & w < \frac{\gamma_s-\gamma_p}{r_p} \\ \frac{1}{2}\log_2(1+\gamma_s), & \text{otherwise} \end{cases} \tag{10}$$

Evidently, R_c is a continuous function with respect to $w \ge 0$ such that the original problem in (7) is equivalent to

$$\begin{aligned} \max_{\rho,w} \quad & R_1(\rho, w) \\ \text{s.t.} \quad & (1-\rho)T - t_c \ge 0 \\ & X\rho T - wt_c \ge 0 \\ & 0 \le \rho \le \frac{Q}{R_pT} \\ & 0 \le w \le \frac{\gamma_s - \gamma_p}{r_p} \end{aligned} \tag{11}$$

According to Theorem 2, the optimization problem in (11) is quasi-convex (with a quasi-concave objective function and convex constraints) and continuous within a closed interval. Thus, the global optimum of (11) exists and the optimal ρ and w can be derived by comparing all the candidate KKT points.

The KKT optimality condition of (11) is given by

$$\begin{cases} \frac{\partial R_1}{\partial \rho} = 0, \quad \frac{\partial R_1}{\partial w} - \lambda_1 + \lambda_2 = 0 \\ (1-\rho)T - t_c > 0, \quad X\rho T - wt_c > 0 \\ 0 < \rho < \frac{Q}{R_pT}, \quad 0 \le w \le \frac{\gamma_s-\gamma_p}{r_p} \\ \lambda_1\left(w - \frac{\gamma_s-\gamma_p}{r_p}\right) = 0, \quad \lambda_2 w = 0 \\ \lambda_1, \lambda_2 \ge 0 \end{cases} \tag{12}$$

Note that the cases of $\rho = 0$, $(1-\rho)T - t_c = 0$, $X\rho T - wt_c = 0$ and $\rho = Q/R_pT$ could be also candidate KKT points of (7). However, obviously the cases of $\rho = 0$, $(1-\rho)T - t_c = 0$ and $X\rho T - wt_c = 0$ lead to null achievable throughput, and the cases $\rho = Q/R_pT$ pertains to non-cooperation mode and are already discussed in last subsection. Therefore, we eliminate the complementary slackness conditions and dual variables concerning theses cases. Specially, we will also prove that the KKT point with $w = 0$ is infeasible in the following part.

1) Candidate KKT point 1: $\lambda_1 = \lambda_2 = 0$: Deriving the optimal ρ and w while $\lambda_1 = \lambda_2 = 0$ is equivalent to solving the following equation system:

$$\begin{cases} \frac{\partial R_1}{\partial \rho} = 0 \\ \frac{\partial R_1}{\partial w} = 0 \end{cases} \tag{13}$$

Theorem 3: The candidate KKT point (ρ_{c1}, w_{c1}) while $\lambda_1 = \lambda_2 = 0$ can be expressed as

$$\begin{cases} \rho_{c1} = \frac{R_{c1}T - Q}{(R_{c1}-R_p)T(W_1+1)} - \frac{C_1 W_1}{K_1(W_1+1)} \\ w_{c1} = \frac{Xr_p - \gamma_p - 1}{r_p W\left(\frac{Xr_p-\gamma_p-1}{\mathrm{e}(1+\gamma_p)^2}\right)} - \frac{\gamma_p+1}{r_p} \end{cases} \tag{14}$$

where

$$\begin{cases} R_{c1} = \frac{1}{2}\log_2(1+\gamma_p + w_{c1}r_p) \\ K_1 = \left((Xr_s - 1)R_{c1} + (w_{c1}r_s + 1)R_p\right)T \\ C_1 = R_{c1}T - (w_{c1}r_s + 1)Q \\ W_1 = W\left(\frac{K_1}{\mathrm{e}(R_{c1}-R_p)T}\right) \end{cases}$$

Proof: Please refer to Appendix E. ■

Then the feasibility of (ρ_{c1}, w_{c1}) can be tested with the constraints in (11).

2) Candidate KKT point 2: $\lambda_2 = 0$ and $\lambda_1 \ge 0$: In this case, we have

$$w_{c2} = \frac{\gamma_s - \gamma_p}{r_p} \tag{15}$$

Similar with the proof of Theorem 3, by defining

$$V_{c2}|_{w=\frac{\gamma_s-\gamma_p}{r_p}} = \frac{(K_a + K_b)\rho + C_a + C_b}{K_a\rho + C_a}$$

and

$$\begin{cases} R_{c2} = \frac{1}{2}\log_2(1+\gamma_s) \\ K_2 = \left((Xr_s - 1)R_{c2} + \left(\frac{(\gamma_s-\gamma_p)r_s}{r_p} + 1\right)R_p\right)T \\ C_2 = R_{c2}T - \left(\frac{(\gamma_s-\gamma_p)r_s}{r_p} + 1\right)Q \\ W_2 = W\left(\frac{K_2}{\mathrm{e}(R_{c2}-R_p)T}\right) \end{cases}$$

ρ_{c2} is given by

$$\rho_{c2} = \frac{R_{c2}T - Q}{(R_{c2} - R_p)T(W_2 + 1)} - \frac{C_2 W_2}{K_2(W_2 + 1)} \tag{16}$$

Then the feasibility of (ρ_{c2}, w_{c2}) can be tested with the constraints in (11). Here, the constraint $\lambda_1 \geq 0$ can be skipped because we have $\lambda_1 = ((1-\rho)T - t_c)t_c/(A+B)$ (A and B as defined in Appendix F) according to the second equation in (12) and it is equivalent to test the constraint $(1-\rho)T - t_c > 0$ instead.

3) Candidate KKT point 3: $\lambda_1 = 0$ and $\lambda_2 \geq 0$: In this case, we have $w_{c3} = 0$. Similar with the proof of Theorem 3, by defining

$$V_{c3}|_{w=0} = \frac{(K_a + K_b)\rho + C_a + C_b}{K_a \rho + C_a}$$

and

$$\begin{cases} R_{c3} = \frac{1}{2}R_p \\ K_3 = \frac{Xr_s+1}{2}R_p T \\ C_3 = \frac{1}{2}R_p T - Q \\ W_3 = W\left(\frac{-Xr_s-1}{\mathrm{e}}\right) \end{cases}$$

ρ_{c3} is given by

$$\rho_{c3} = \frac{2Q - R_p T}{R_p T(W_3 + 1)} - \frac{C_3 W_3}{K_3(W_3 + 1)} \tag{17}$$

Similarly, the feasibility of (ρ_{c3}, w_{c3}) can be tested with the constraints in (11). However, it is noteworthy that W_3 is a complex for positive X and r_s according to the properties of Lambert W function ($W(x)$ is complex while $x < -1/\mathrm{e}$ [34]). Therefore, it can be concluded that (ρ_{c3}, w_{c3}) is practically infeasible. In fact, the infeasibility of $w = 0$ also indicates that it is superfluous for the SU to allocate null power for cooperative relay following the DF protocol.

Hence, by comparing $R_1(\rho_{c1}, w_{c1})$ and $R_1(\rho_{c2}, w_{c2})$, the SU's optimal save-ratio and allocated power for cooperative relay can be expressed as

$$(\rho_c^*, w_c^*) = \underset{(\rho,w)\in\{(\rho_{c1},w_{c1}),(\rho_{c2},w_{c2})\}}{\arg\max} R_1(\rho, w) \tag{18}$$

VI. Numerical Results

In this section, we illustrate how the optimal strategy depends on the system parameters in both cooperation and non-cooperation modes.

A. Non-Cooperation Mode

According to (8) and (9), the optimal save-ratio in non-cooperation mode is only dependent on Xr_s and Q/R_pT. Fig. 5 numerically shows the optimal save-ratio with different Xr_s and Q/R_pT. It can be seen that as either X or r_s increases, the optimal strategy in non-cooperation mode tends to be allocating a smaller fraction of time for energy harvesting. Meanwhile, it also shows that Q/R_pT works as a lower-bound of the optimal save-ratio in non-cooperation mode.

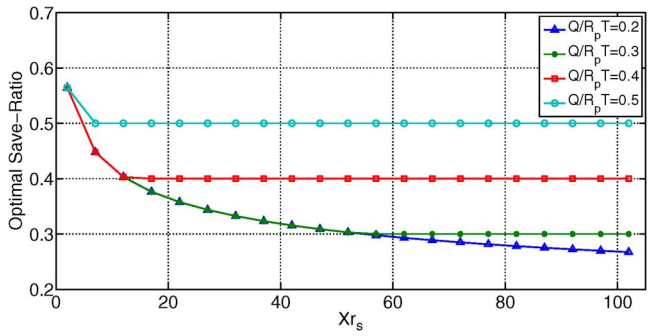

Fig. 5. Optimal save-ratio in non-cooperation mode with different Xr_s and Q/R_pT.

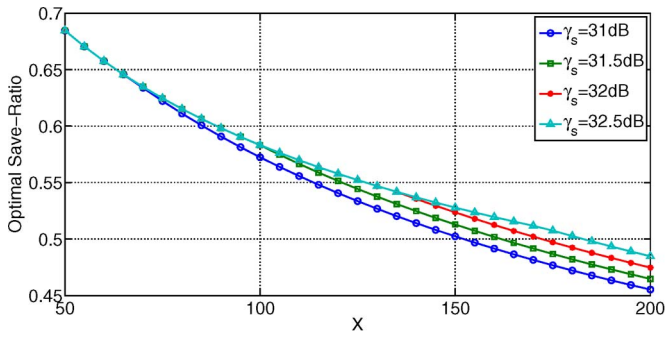

Fig. 6. Optimal save-ratio in cooperation mode with different X and γ_s.

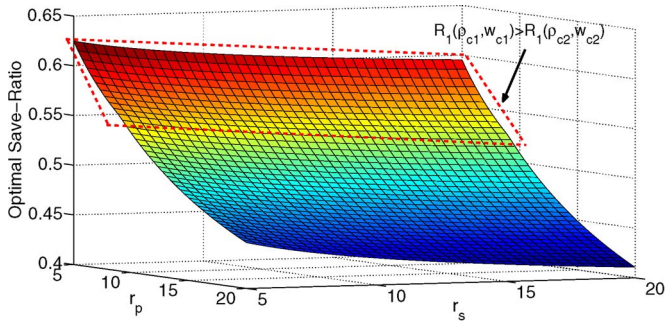

Fig. 7. Optimal save-ratio in cooperation mode with different r_p and r_s.

B. Cooperation Mode

In this subsection, we numerically evaluate the optimal save-ratio and allocated power for cooperative relay in cooperation mode by setting $Q = 3$, $T = 1$, and $R_p = 4$ (namely, optimal save-ratio is upper-bounded with 0.75).

Optimal Save-Ratio: Optimal save-ratio in cooperation mode with different system parameters is shown in Figs. 6 and 7, respectively. In Fig. 6, we can see that the optimal save-ratio decreases as X increases, which is similar with the case in non-cooperation mode. However, along with the growth of γ_s, the optimal save-ratio increases. This is because with a better channel condition for cooperative relay, the optimal strategy tends to harvest more energy such that more power could be allocated for cooperative relay. Fig. 7 shows the optimal save-ratio with different r_p and r_s. We can see that the optimal save-ratio decreases as r_p and r_s increase and drops faster with the growth of r_p. The red dotted rectangle in Fig. 7 indicates the area within which $R_1(\rho_{c1}, w_{c1}) > R_1(\rho_{c2}, w_{c2})$.

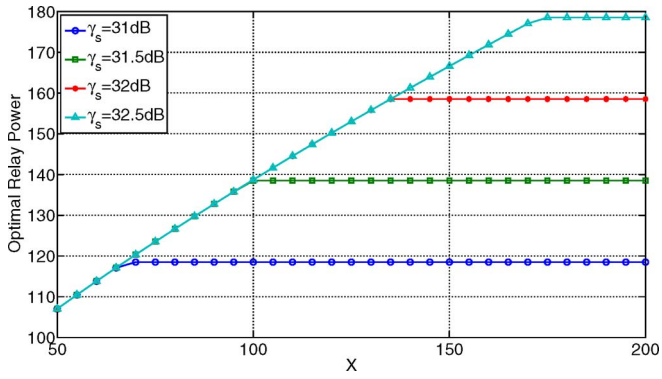

Fig. 8. Optimal allocated power for cooperative relay in cooperation mode with different X and γ_s.

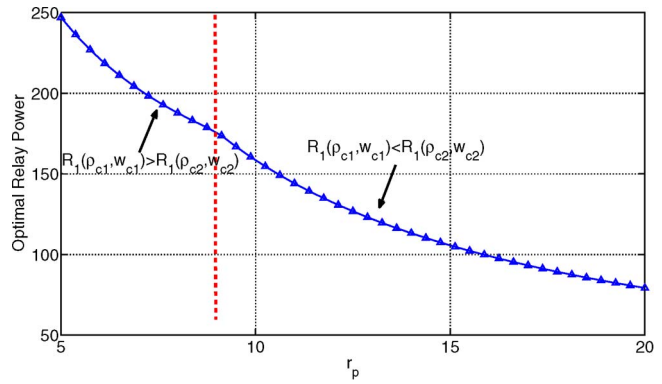

Fig. 9. Optimal allocated power for cooperative relay in cooperation mode with different r_p.

Optimal Allocated Power for Cooperative Relay: Optimal allocated power for cooperative relay in cooperation mode with different system parameters is shown in Figs. 8 and 9, respectively. In Fig. 8, the optimal allocated power for cooperative relay presents a linearly proportional dependency of X and is upper-bounded with $(\gamma_s - \gamma_p)/r_p$. Similar with what is previously discussed, this is because the optimal strategy tends to allocate more power for cooperative relay with a better channel condition. Since the optimal allocated power for cooperative relay is irrespective of r_s according to (14) and (15), we only illustrate the optimal save-ratio with different r_p in Fig. 9. Surprisingly, it shows that as r_p increases, the optimal strategy in cooperation mode tends to allocate less power for cooperative relay, which implies that enough energy must be conserved for secondary transmission even with better channel condition for cooperative relay. Moreover, "$R_1(\rho_{c1}, w_{c1}) > R_1(\rho_{c2}, w_{c2})$" area and "$R_1(\rho_{c1}, w_{c1}) < R_1(\rho_{c2}, w_{c2})$" area are separated by the red dotted cutting line in Fig. 9.

VII. Optimal Decision and Protocol Design

In this section, based on the theoretical analysis in Section V, we perform in-depth analysis on how to make the optimal decision (to cooperate with the PU or not) and further propose the optimal cooperation protocol (OCP), which first separately derives the optimal solutions for both non-cooperation mode (optimal save-ratio) and cooperation mode (optimal save-ratio and allocated power for cooperative relay), then makes the optimal decision by comparing the two solutions with a simple two-level test.

A. Optimal Decision

For the non-cooperation mode, the optimal save-ratio ρ_{nc}^* can be easily derived according to (9). For the cooperation mode, the optimal solution (ρ_c^*, w_c^*) can be derived by comparing the optimal achievable throughput of the two KKT candidate points. Finally, the optimal decision can be made by comparing the optimal achievable throughput in the two modes ($R_0(\rho_{nc}^*)$ and $R_1(\rho_c^*, w_c^*)$).

We define

$$\begin{cases} A_c = (1-\rho_c^*)\,T - t_c^*, & B_c = (X\rho_c^* T - w_c^* t_c^*) \\ A_{nc} = (1-\rho_{nc}^*)\,T, & B_c = X\rho_{nc}^* T \end{cases} \tag{19}$$

where $t_c^* = (Q - R_p\rho_c^* T)/R_c^*$ and $R_c^* = (1/2)\log_2(1+\gamma_p + w_c^* r_p)$, then we have

$$\begin{cases} R_0\left(\rho_{nc}^*\right) = A_{nc}\log_2\left(1+\frac{B_{nc}r_s}{A_{nc}}\right) \\ R_1\left(\rho_c^*, w_c^*\right) = A_c\log_2\left(1+\frac{B_c r_s}{A_c}\right) \end{cases} \tag{20}$$

By using the approximation $\log_2(1+x) \approx \sqrt{x}$ [36], comparing $R_0(\rho_{nc}^*)$ and $R_1(\rho_c^*, w_c^*)$ is equivalent to comparing $A_{nc}B_{nc}$ and A_cB_c.

The difference between $A_{nc}B_{nc}$ and A_cB_c, which can be considered as a quadratic function with respect to t_c^*, is given by

$$\begin{aligned} D\left(t_c^*\right) &= A_cB_c - A_{nc}B_{nc} \\ &= w_c^* t_c^{*2} - \left((1-\rho_c^*)Tw_c^* + X\rho_c^* T\right)t_c^* \\ &\quad + \left(\rho_{nc}^* - \rho_c^*\right)\left(\rho_{nc}^* + \rho_c^* - 1\right)XT^2 \end{aligned} \tag{21}$$

(21) shows that $D(t_c^*)$ is convex since $w_c^* > 0$ and its discriminant can be expressed as

$$\Delta = \left((1-\rho_c^*)\,Tw_c^* - X\rho_c^* T\right)^2 + 4\left(1-\rho_{nc}^*\right)\rho_{nc}^* w_c^* XT^2 \tag{22}$$

Obviously, we have $\Delta > 0$, which indicates that (21) has two different roots. We further define

$$t_c' = \frac{(1-\rho_c^*)\,T}{2} + \frac{X\rho_c^* T}{2w_c^*}$$

at which $D(t_c^*)$ attains its minimum. Then according to the first two constraints in (12), we have $0 < t_c^* < t_c'$.

According to (21), we have $D(0) = (\rho_{nc}^* - \rho_c^*)(\rho_{nc}^* + \rho_c^* - 1)XT^2$. While $\rho_{nc}^* + \rho_c^* \le 1$, $D(0) \le 0$, then we have $D(t_c^*) < 0$, namely, $R_0(\rho_{nc}^*) > R_1(\rho_c^*, w_c^*)$, which can be graphically interpreted by the left part of Fig. 10. While $\rho_{nc}^* + \rho_c^* > 1$, $D(0) > 0$ and the sign of $D(t_c^*)$ can be determined by comparing t_c^* with the lower root of (21), which is given by

$$t_l = \frac{(1-\rho_c^*)Tw_c^* + X\rho_c^* T - \sqrt{\Delta}}{2w_c^*}$$

As is shown in the right part of Fig. 10, when $t_c^* > t_l$, we have $D(t_c^*) < 0$, namely, $R_0(\rho_{nc}^*) > R_1(\rho_c^*, w_c^*)$, otherwise we have $D(t_c^*) \ge 0$ and $R_0(\rho_{nc}^*) \le R_1(\rho_c^*, w_c^*)$.

B. Protocol Design

Based on the previous analytical results, we further propose the optimal cooperation protocol (OCP), the flowchart of which

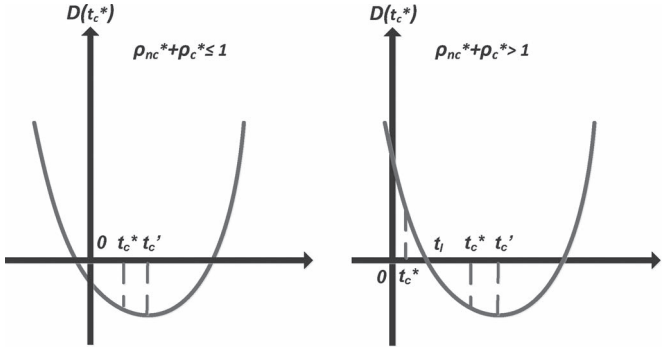

Fig. 10. Graphical interpretation for the sign of $D(t_c^*)$.

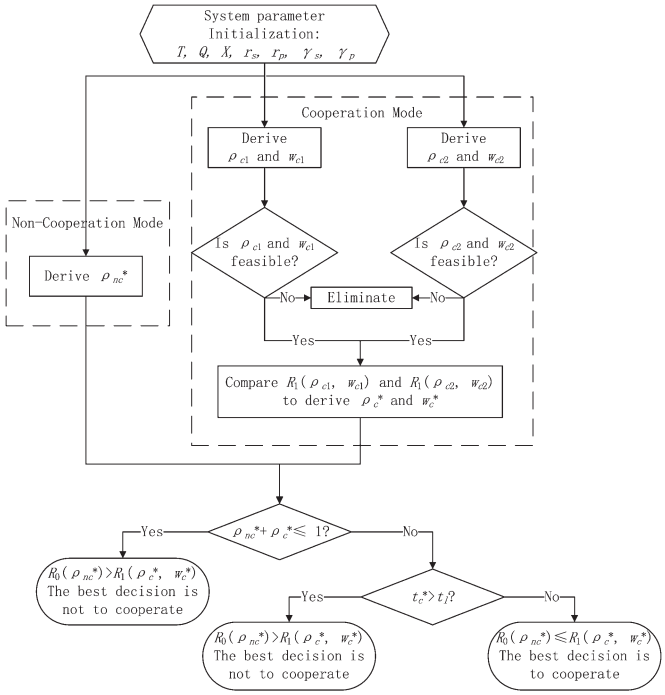

Fig. 11. Flowchart of the OCP.

is shown in Fig. 11. First, ρ_{nc}^* in non-cooperation mode and (ρ_c^*, w_c^*) in cooperation mode are calculated separately. Then $\rho_{nc}^* + \rho_c^*$ is used for the first-level test. While $\rho_{nc}^* + \rho_c^* \leq 1$, the best decision is to operate in non-cooperation mode. While $\rho_{nc}^* + \rho_c^* > 1$, comparison between t_c^* and t_l acts as the second-level test. While $t_c^* > t_l$, the best decision is to operate in non-cooperation mode, otherwise the best decision is to operate in cooperation mode.

Evidently, the OCP shown in Fig. 11 involves comparison between only four candidate optimal points (two for the non-cooperation mode and two for the cooperation mode), which can be readily derived based on the analytical results in Section V. Since the proposed protocol is based on the closed-form solution to the achievable throughput maximization problem, it can derive the optimal solution once for all and make the optimal decision through a simple two-level test while keeping off the non-trivial computational complexity and non-global optimality that could be incurred by other searching-based optimization algorithms.

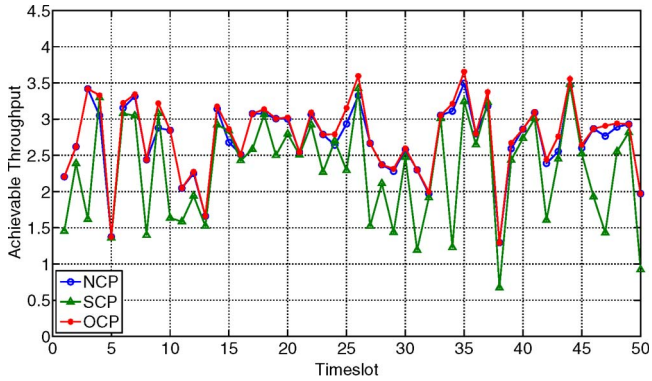

Fig. 12. Achievable throughput trace in share case with $X \sim \Gamma(10, 5)$ and $\gamma_s \sim \text{Exp}(1/500)$.

VIII. Performance Evaluation

A. Methodology

In this section, by achievable throughput simulation over 50 timeslots, we compare the performance of the proposed optimal cooperation protocol with that of the other two protocols: the non-cooperation protocol (NCP), in which the SU starts its transmission only after the PU's transmission is completed (namely $\rho = Q/R_pT$), and the stochastic cooperation protocol (SCP), in which the SU cooperates with the PU with randomly selected save-ratio and randomly allocated power for cooperative relay. For the system parameters, we assume that X is Gamma-distributed (since Gamma distribution can model many positive random variables [37] and the extension work of [24] has precedentedly used Gamma distribution to model energy harvesting rate). The probability distribution of X is given by

$$f(x) = \frac{x^{k-1}}{\theta^k \Gamma(k)} \mathrm{e}^{-\frac{x}{\theta}},\ x > 0$$

where k, $\theta > 0$ and $\Gamma(.)$ refer to the shape parameter, scale parameter and gamma function, respectively. Moreover, we consider a Rayleigh fading channel such that γ_s, r_p and r_s are exponential-distributed (since squaring a Rayleigh-distributed random variable results in an exponential-distributed one [38]). Take γ_s for example, the probability distribution is given by

$$f(\gamma_s) = \lambda \mathrm{e}^{-\lambda \gamma_s},\ \gamma_s > 0$$

where λ refers to the rate parameter. In each timeslot, system parameters are randomly generated according to their respective probability distributions. In addition, two cases with different PU traffic are investigated: the "share" case, in which the PU is able to complete its transmission within one timeslot even without the SU's cooperation (namely, $Q < R_pT$), and the "monopoly" case, in which the PU monopolizes the licensed channel all the time (namely, $Q = R_pT$).

B. Share Case

In share case, we set $Q = 3$, $T = 1$ and $R_p = 4$ with $r_p \sim \text{Exp}(20)$ and $r_s \sim \text{Exp}(20)$. The simulation results (50-timeslot achievable throughput traces) with different probability distributions of X and γ_s are shown in Figs. 12–14. It can be seen that in each timeslot, OCP outperforms both NCP and SCP. We also count up the number of times when the optimal decision in

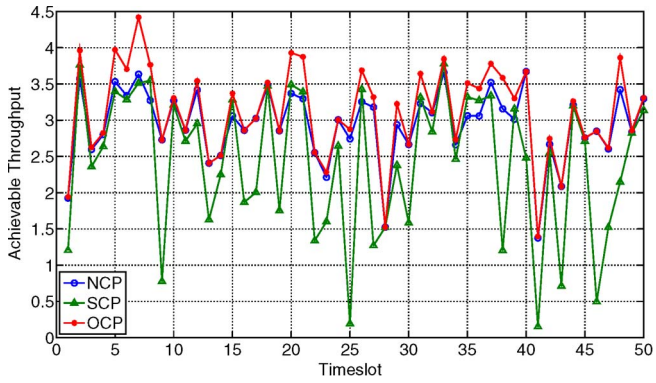

Fig. 13. Achievable throughput trace in share case with $X \sim \Gamma(20, 5)$ and $\gamma_s \sim \text{Exp}(1/1000)$.

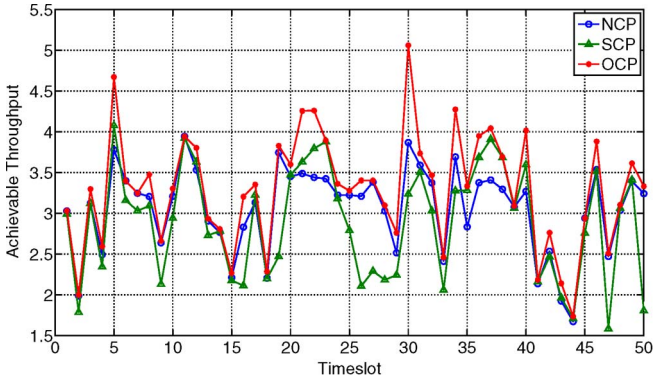

Fig. 14. Achievable throughput trace in share case with $X \sim \Gamma(30, 5)$ and $\gamma_s \sim \text{Exp}(1/1500)$.

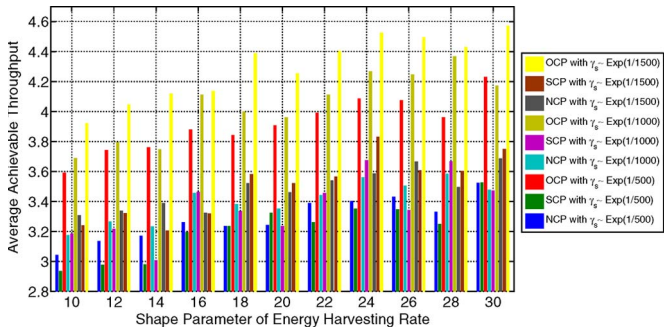

Fig. 15. Average achievable throughput in share case with different probability distribution of X and γ_s.

OCP is to cooperate and the statistics shows that as X and γ_s grow, the optimal decision tends to be operating in the cooperation mode of OCP (30 times in Fig. 12, 40 times in Fig. 13 and 46 times in Fig. 14, respectively). This is because either more harvested energy or better channel condition for cooperative relay makes OCP inclined to cooperate with the PU. Moreover, we also investigate the average achievable throughput in each simulation (over 50 timeslots) with different probability distributions of X and γ_s, as shown in Fig. 15. Here, we alter the shape parameter of distribution of X (while the scale parameter remains constant) and the rate parameter of distribution of γ_s to alter their expectations (because the expectation of a Gamma-distributed random variable is the product of shape and scale parameters and that of an exponential-distributed one is the inverse of rate parameter). We can see that higher X and γ_s

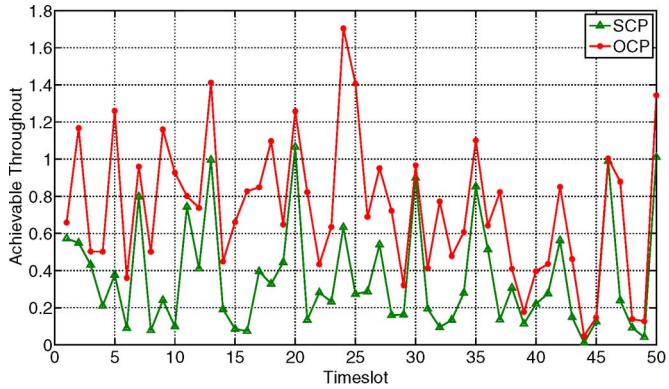

Fig. 16. Achievable throughput trace in monopoly case with $X \sim \Gamma(10, 5)$ and $\gamma_s \sim \text{Exp}(1/500)$.

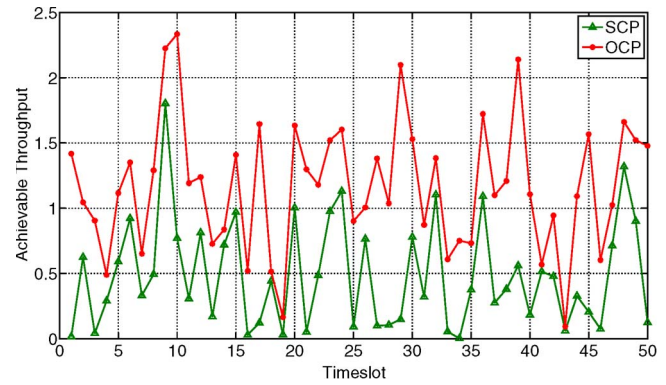

Fig. 17. Achievable throughput trace in monopoly case with $X \sim \Gamma(20, 5)$ and $\gamma_s \sim \text{Exp}(1/1000)$.

lead to higher achievable throughput and stronger performance gain of OCP over NCP and SCP. Another interesting finding is that the performance of SCP is even worse than that of NCP, especially for lower X and γ_s), which implies that with less harvested energy or worse channel condition for cooperative relay, the SU cannot benefit from cooperation at random, instead, operating in non-cooperation mode could be even better.

C. Monopoly Case

In monopoly case, to investigate how much throughput can be squeezed out while the PU monopolizes the licensed channel all the time, we set $Q = 4$, $T = 1$ and $R_p = 4$ with $r_p \sim N(10, 2)$ and $r_s \sim N(10, 2)$. Here, only SCP is involved for performance comparison since apparently NCP results in null achievable throughput in monopoly case. The simulation results (50-timeslot achievable throughput traces) with different probability distributions of X and γ_s are shown in Figs. 16–18. It can be shown that OCP outperforms SCP in each single timeslot and the performance gain is much higher than that in share case. In a similar way with share case, we investigate the average achievable throughput in each simulation (over 50 timeslots) with different probability distributions of X and γ_s, as shown in Fig. 19. We can see that in monopoly case, SCP's performance improvement from higher X is very limited especially with lower γ_s while OCP can still squeeze out considerable throughput and significantly outperforms SCP especially with higher γ_s since it fully utilizes the information of system parameter to make the optimal decision.

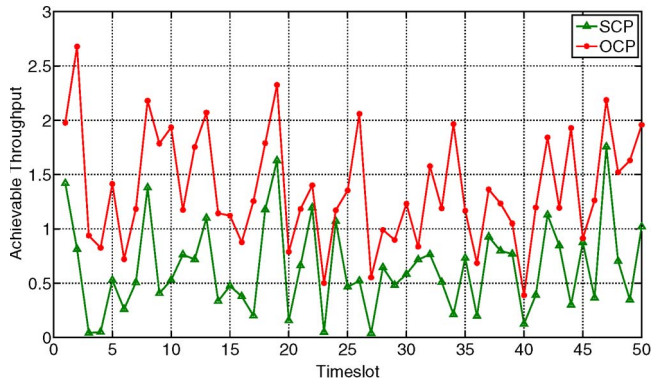

Fig. 18. Achievable throughput trace in monopoly case with $X \sim \Gamma(30, 5)$ and $\gamma_s \sim \text{Exp}(1/1500)$.

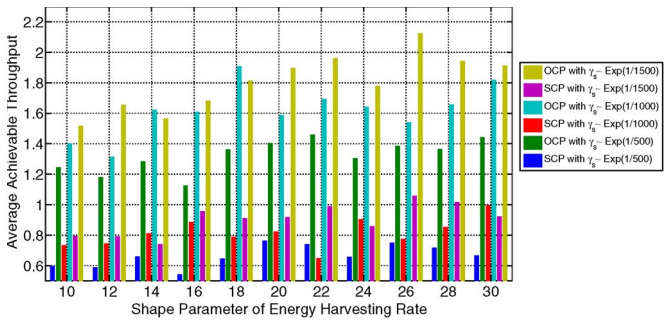

Fig. 19. Average achievable throughput in monopoly case with different probability distribution of X and γ_s.

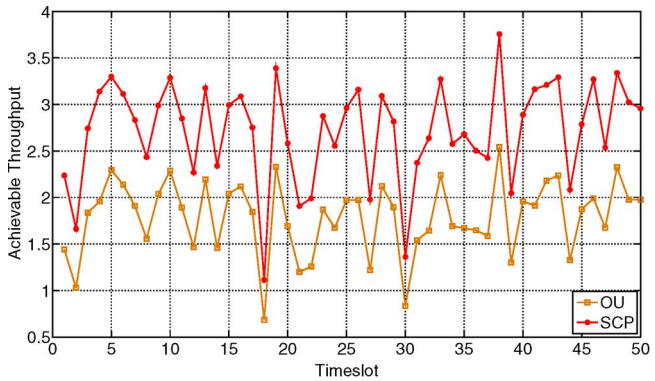

Fig. 20. Achievable throughput trace in share case with $X \sim \Gamma(10, 5)$ and $\gamma_s \sim \text{Exp}(1/500)$.

D. Comparison With Underlay Transmission

We also compare the performance of OCP with that of underlay transmission mode, a non-cooperation mode in which the SU is allowed to transmit while the PU is on transmission. The optimal underlay (OU) transmission mode for the SU, where the optimal save-ratio is derived following (8), is considered and we specify that the SU achieves null throughput during collision with the PU.[2] Since the SU achieves nothing if the PU monopolizes the licensed channel all the time, we only consider share case with the same setting in Section VIII-B in this part. The simulation results (50-timeslot achievable

[2]Recent advances that allow SUs to simultaneously relay PUs' data and transmit its own data is not consider in this paper (e.g., multi-antenna SU in [8]).

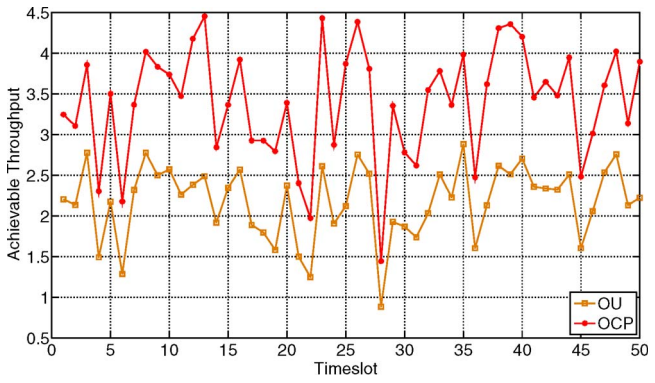

Fig. 21. Achievable throughput trace in share case with $X \sim \Gamma(20, 5)$ and $\gamma_s \sim \text{Exp}(1/1000)$.

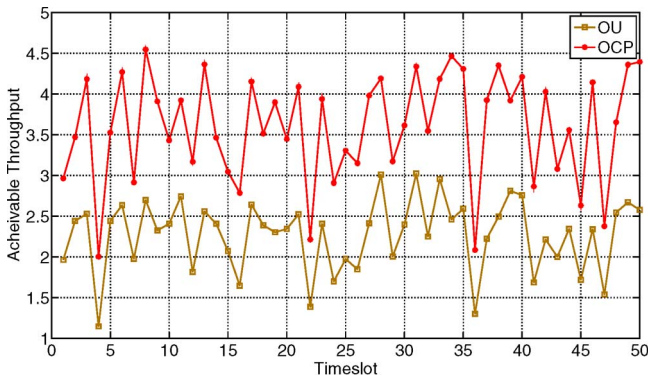

Fig. 22. Achievable throughput trace in share case with $X \sim \Gamma(30, 5)$ and $\gamma_s \sim \text{Exp}(1/1500)$.

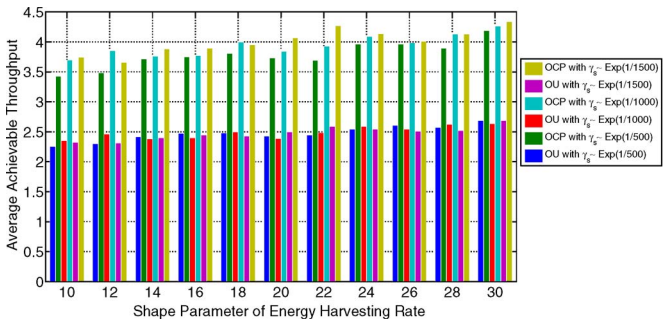

Fig. 23. Average achievable throughput in share case with different probability distribution of X and γ_s.

throughput traces) with different probability distributions of X and γ_s are shown in Figs. 20–22. It can be shown that the performance of OCP is significantly higher than that of OU transmission mode in each single timeslot. This is because in the OU transmission mode, the SU's save-ratio is optimized only for its own transmission regardless of inevitable collision with the PU. Similarly, we investigate the average achievable throughput in each simulation (over 50 timeslots) with different probability distributions of X and γ_s, as shown in Fig. 23. We can see that the performance improvement of OU transmission mode from higher X is very limited due to frequent collision with the PU. On the contrary, the OCP still utilizes higher X to improve the SU's achievable throughput since it makes the optimal decision on to cooperate with the PU or not and collision with the PU never happens.

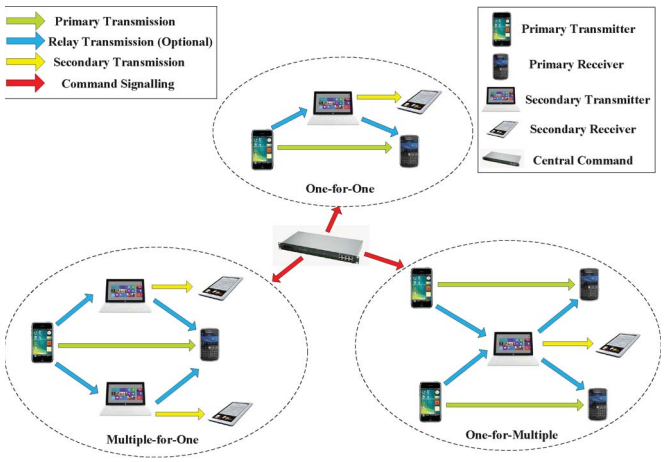

Fig. 24. Cooperation in CR networks with multiple PUs and SUs.

IX. Discussion

Since the proposed OCP is based on the closed-form solution to the achievable throughput maximization problem, the optimal cooperation strategy can be readily derived according to the analysis in Section V and VII. However, in order for practical implementation, the SU must be capable of acquiring PUs' information as well as channel parameters (as shown in Table I). In addition to single-PU-singe-SU ("one-for-one") systems, applying the OCP to large-scale multi-PU-multi-SU networks could be more complicated due to the huge number of PUs and SUs. Therefore, in this section, we briefly discuss concerns and challenges while implementing the OCP in a practical network.

A. Concerns in Implementation

Evidently, exchanging information between primary and secondary systems with overhead signaling inevitably bring about additional spectrum usage. In this sense, we propose that the CR system implementing the OCP shall be customized for a specific primary system with which the CR system shares licensed spectrum. In other words, the operating protocol of the specific primary system shall be known ahead of time by the secondary system such that no additional information exchange to acquire PUs' information is necessary. For instance, if a CR system is designed to share spectrum with a GSM system, the OCP should be implemented with $T = 0.577$ ms, $Q = 156.25$ bit and $R_p = 270.833$ kbit/s.

Likewise, acquiring channel parameters in the proposed OCP requires additional effort from the secondary system. If highly complex channel estimation is individually performed by each SU, non-negligible consumption in time and energy is inevitably incurred. To tackle this concern, we propose that the CR system shall operate in a centralized manner, whereby all the SUs acquire the channel parameters from a central entity (e.g., the cognitive base station in [39]). As shown in Fig. 24, the entity shall be capable of exchanging information with the primary system and performing channel estimation for the whole secondary system as well as making decisions as a central command (e.g., cooperation strategy of each SU).

B. Challenges in Large-scale Networks

To implement the proposed OCP in a practical network with multiple PUs and SUs, a primary challenge to be faced with is the cooperation assignment problem, namely, by what rules each SU is assigned to its corresponding PU as a cooperative relay in order to optimize the collective performance of the entire CR network (e.g., overall achievable throughput) rather than the individual performance as discussed in this paper. As shown in Fig. 24, since the number of PUs and SUs in a practical network are unnecessarily equal with each other, there could be cases where multiple SUs serve as the relays for one PU ("multiple-for-one") or one SU serves as the relay for multiple PUs ("one-for-multiple"). Therefore, the optimal cooperation strategies in those cases are still to be further investigated.

Another challenging issue in large-scale networks is the complexity of cooperation assignment. Based on the optimal cooperation strategy in "one-for-one" case discussed in this paper as well as that in the aforementioned "multiple-for-one" and "one-for-multiple" cases, cooperation assignment problem can be intuitively formulated as a binary integer programming (where the variables are the binary assignment indicators). For a small-scale network with less PUs and SUs, exhaustive searching through all the possible assignment cases could be feasible, which however, is intractable for a large-scale network with an enormous number of PUs and SUs. In this sense, low-complexity algorithms for cooperation assignment in large-scale networks are necessarily to be investigated.

X. Conclusion

In this paper, we consider a CR system with one PU and one SU and both of their transmitters operate in time-slotted mode. The SU, which has no fixed power supplies and extracts energy exclusively via energy harvested from ambient radio signal, can optionally cooperate with the PU to improve PU's throughput such that more opportunities can be available for its own transmission. To tackle the tradeoffs in energy harvesting, cooperative relay and secondary transmission, we separately investigate the optimal action in non-cooperation and cooperation modes to maximize the SU's achievable throughout and derive the optimal closed-form solutions with numerical analysis. Based on the analytical results, we further propose the optimal cooperation protocol (OCP), which simply involves a two-level test, to make the optimal cooperation decision (whether to cooperate with the PU or not). Simulation results show that the OCP we propose outperforms the other two protocols (non-cooperation protocol and stochastic cooperation protocol) in both "share case" (in which the PU is able to complete its transmission within one timeslot even without the SU's cooperation) and "monopoly case" (in which the PU monopolizes the licensed channel all the time). In addition, we also show that the proposed OCP significantly outperforms the optimal underlay transmission mode (in which the SU is allowed to transmit while the PU is on transmission).

APPENDIX A
PROOF OF LEMMA 1

Evidently, (4) is a continuous function while $0 < \rho < 1$. Therefore, we investigate the second derivative of (4) to testify its concavity.

The first derivative can be expressed as

$$\frac{\partial R_0}{\partial \rho} = -\log_2\left(1+\frac{Xr_s\rho}{1-\rho}\right) + \frac{Xr_s}{\ln 2\left((Xr_s-1)\rho+1\right)} \tag{23}$$

Then the second derivative can be further derived

$$\begin{aligned}\frac{\partial^2 R_0}{\partial \rho^2} &= -\frac{1}{\ln 2}\left(\frac{Xr_s}{(1-\rho)\left((Xr_s-1)\rho+1\right)}\right.\\ &\qquad \left.-\frac{Xr_s(Xr_s-1)}{\left((Xr_s-1)\rho+1\right)^2}\right)\\ &= \frac{-(Xr_s)^2}{\ln 2(1-\rho)\left((Xr_s-1)\rho+1\right)^2}\end{aligned} \tag{24}$$

Thus, for $X > 0$ and $0 \le \rho \le 1$, we have

$$\frac{\partial^2 R_0}{\partial \rho^2} < 0$$

which proves the concavity of (4) for $0 \le \rho \le 1$.

APPENDIX B
PROOF OF THEOREM 1

We denote the stationary point of (4) by ρ_0^* and consequently we have

$$\left.\frac{\partial R_0}{\partial \rho}\right|_{\rho=\rho_0^*} = 0$$

It can be inferred from Lemma 1 that $R_0(\rho)$ attains the global optimality at ρ_0^* for $0 \le \rho \le 1$.

We define

$$V_{nc} = \frac{(Xr_s-1)(1-\rho)}{(Xr_s-1)\rho+1}$$

Then ρ_0^* can be derived as follows:

$$\begin{aligned}&-\log_2\left(1+\frac{Xr_s\rho}{1-\rho}\right) + \frac{Xr_s}{\ln 2\left((Xr_s-1)\rho+1\right)} = 0\\ &\Rightarrow \ln\left(\frac{(Xr_s-1)\rho+1}{1-\rho}\right) = \frac{Xr_s}{(Xr_s-1)\rho+1}\\ &\Rightarrow \ln V_{nc} = -V_d + \ln(Xr_s-1) - 1\\ &\Rightarrow \rho_0^* = \frac{Xr_s - 1 - W\left(\frac{Xr_s-1}{\mathrm{e}}\right)}{(Xr_s-1)\left(W\left(\frac{Xr_s-1}{\mathrm{e}}\right)+1\right)}\end{aligned} \tag{25}$$

APPENDIX C
PROOF OF LEMMA 3

Obviously, $f(A,B)$ is a monotonically increasing function over B for $B > 0$. Hence, we only focus on proving the increasing monotonicity of $f(A,B)$ over A for $A > 0$.

The first derivative of $f(A,B)$ with respect to A can be expressed as

$$\frac{\partial f(A,B)}{\partial A} = \ln\left(1+\frac{B}{A}\right) - \frac{B}{A+B} \tag{26}$$

According to the property of natural logarithm, we have $\ln(1+x) > x/(1+x)$ for $X > 0$, then it can be derived that $\partial f(A,B)/\partial A > 0$. Therefore, $f(A,B)$ is a monotonically increasing function for $A, B > 0$.

APPENDIX D
PROOF OF THEOREM 2

We define the following variables to facilitate the derivation:

$$\begin{cases} A = (1-\rho)T - t_c = K_a\rho + C_a \\ B = (X\rho T - wt_c)r_s = K_b\rho + C_b \end{cases} \tag{27}$$

where

$$\begin{cases} K_a = \left(\frac{R_p}{R_c}-1\right)T, \quad C_a = T - \frac{Q}{R_c} \\ K_b = \left(X + w\frac{R_p}{R_c}\right)Tr_s, \quad C_b = -\frac{wQr_s}{R_c} \end{cases} \tag{28}$$

and the SU's achievable throughput can be rewritten as $R_1(\rho, w) = A\log_2(1+B/A)$.

Since $g(B) = \log_2(1+B)$ is concave for $B > 0$ and perspective operation preserves concavity [35], the perspective function of $g(B)$, which is defined by

$$f(A,B) = A\log_2\left(1+\frac{B}{A}\right)$$

is also concave for $A, B > 0$.

Apparently, both A and B are concave over ρ since they are linear functions with respect to ρ. Similarly, according to (10), R_c is a constant while $w \ge (\gamma_s - \gamma_p)/r_p$ such that both A and B are concave over w since they are linear functions with respect to w. Since the inverse of logarithm function is convex for $x > 1$[3] and composition with affine mapping preserve convexity [35], $1/R_c$ is a convex function of w while $w < (\gamma_s - \gamma_p)/r_p$. A can be rewritten as

$$A = \frac{R_p\rho T - Q}{R_c}$$

Since we have $\rho \le Q/R_pT$ in cooperation mode, A is concave over w for $0 \le w < (\gamma_s - \gamma_p)/r_p$. Similarly, while $0 \le w < (\gamma_s - \gamma_p)/r_p$, B can be rewritten as

$$B = (R_p\rho T - Q)r_s\frac{w}{R_c} + X\rho T r_s$$

Here, w/R_c is quasi-convex over w since R_c is concave [35]. Since we have $\rho \le Q/R_pT$ in cooperation mode, B is quasi-concave and $B \ge 0$ can be replaced by

$$w - \frac{X\rho T}{Q - R_p\rho T}R_c \le 0$$

Therefore, the constraint $B \ge 0$ is convex.

[3]The convexity of the inverse of logarithm function ($f(x) = 1/\ln(x)$) can be verified by investigating its second-order derivative.

According to Lemma 2 and the composition theorem for quasi-convex functions [35], it can be concluded that the problem in (7) is convex over ρ and w for $0 \le \rho \le Q/R_pT$ and $w \ge (\gamma_s - \gamma_p)/r_p$, while quasi-convex over w for $0 \le w < (\gamma_s - \gamma_p)/r_p$.

APPENDIX E
PROOF OF THEOREM 3

Let A'_ρ, A'_w, B'_ρ, B'_w denote the first-order partial derivatives ("$'$" denotes the first-order derivative in the following part) of A and B, then (13) can be rewritten as

$$\begin{cases} A'_\rho \ln\left(1+\frac{B}{A}\right) + \frac{B'_\rho A - A'_\rho B}{A+B} = 0 \\ A'_w \ln\left(1+\frac{B}{A}\right) + \frac{B'_w A - A'_w B}{A+B} = 0 \end{cases} \tag{29}$$

From the first equation of (29), it can be derived that

$$\ln\left(1+\frac{B}{A}\right) = \frac{A'_\rho B - B'_\rho A}{A'_\rho (A+B)} \tag{30}$$

Combing (30) with the second equation of (29), we have

$$\frac{B'_\rho}{A'_\rho} = \frac{B'_w}{A'_w}$$

Then w_{c1} can be derived as follows:

$$\begin{aligned} &\frac{XR_c + wRp}{R_p - R_c} = w - \frac{R_c}{R'_c} \\ &\Rightarrow R_c = (X+w)R'_c + R_p \\ &\Rightarrow \ln(1+\gamma_p + wr_p) = \frac{(X+w)r_p}{1+\gamma_p+wr_p} + 2\ln(2)R_p \\ &\Rightarrow w_{c1} = \frac{Xr_p - \gamma_p - 1}{r_p W\left(\frac{Xr_p-\gamma_p-1}{\mathrm{e}(1+\gamma_p)^2}\right)} - \frac{\gamma_p+1}{r_p} \end{aligned} \tag{31}$$

The first equation of (29) can rewritten as

$$K_a \ln\left(\frac{(K_a+K_b)\rho + C_a + C_b}{K_a\rho + C_a}\right) + \frac{K_bC_a - K_aC_b}{(K_a+K_b)\rho + C_a + C_b} = 0 \tag{32}$$

We define

$$V_{c1}|_{w=w_{c1}} = \frac{(K_a+K_b)\rho + C_a + C_b}{K_a\rho + C_a}$$

and

$$\begin{cases} R_{c1} = \frac{1}{2}\log_2(1+\gamma_p + w_{c1}r_p) \\ K_1 = \left((Xr_s - 1)R_{c1} + (w_{c1}r_s + 1)R_p\right)T \\ C_1 = R_{c1}T - (w_{c1}r_s + 1)Q \\ W_1 = W\left(\frac{K_1}{\mathrm{e}(R_{c1}-R_p)T}\right) \end{cases}$$

Then ρ_{c1} can be derived as follows:

$$\begin{aligned} &K_a \ln V_{c1} = \frac{K_aC_b - K_bC_a}{(K_a+K_b)\frac{-C_aV_{c1}+C_a+C_b}{K_aV_{c1}-K_a-K_b} + C_a + C_b} \\ &\Rightarrow \ln V_{c1} = 1 - \frac{K_a+K_b}{K_aV_{c1}} \\ &\Rightarrow V_{c1} = \frac{K_1}{(R_{c1}-R_p)W_1} \\ &\Rightarrow \rho_{c1} = \frac{R_{c1}T - Q}{(R_{c1}-R_p)T(W_1+1)} - \frac{C_1W_1}{K_1(W_1+1)} \end{aligned} \tag{33}$$

ACKNOWLEDGMENT

We would also like to express our gratitude toward Prof. W. Ai from Beijing University of Posts and Telecommunications and Prof. X. Cheng from the George Washington University for their technical support.

REFERENCES

[1] B. Wang, Y. Wu, F. Han, Y.-H. Yang, and K. J. R. Liu, "Green wireless communications: A time-reversal paradigm," *IEEE J. Sel. Areas Commun.*, vol. 29, no. 8, pp. 1698–1710, Sep. 2011.
[2] S. Sudevalayam and P. Kulkarni, "Energy harvesting sensor nodes: Survey and implications," *IEEE Commun. Surveys Tuts.*, vol. 13, no. 3, pp. 443–461, 2011.
[3] Q. Zhang, J. Jia, and J. Zhang, "Cooperative relay to improve diversity in cognitive radio networks," *IEEE Commun. Mag.*, vol. 47, no. 2, pp. 111–117, Feb. 2009.
[4] O. Simeone, Y. Bar-Ness, and U. Spagnolini, "Stable throughput of cognitive radios with and without relaying capability," *IEEE Trans. Commun.*, vol. 55, no. 12, pp. 2351–2360, Dec. 2007.
[5] J. Zhang and Q. Zhang, "Stackelberg game for utility-based cooperative cognitiveradio networks," in *Proc. 10th ACM Int. Symp. MobiHoc*, New York, NY, USA, 2009, pp. 23–32.
[6] O. Simeone *et al.*, "Spectrum leasing to cooperating secondary *ad hoc* networks," *IEEE J. Sel. Areas Commun.*, vol. 26, no. 1, pp. 203–213, Jan. 2008.
[7] I. Krikidis, J. N. Laneman, J. S. Thompson, and S. Mclaughlin, "Protocol design and throughput analysis for multi-user cognitive cooperative systems," *IEEE Trans. Wireless Commun.*, vol. 8, no. 9, pp. 4740–4751, Sep. 2009.
[8] R. Manna, R. H. Y. Louie, Y. Li, and B. Vucetic, "Cooperative spectrum sharing in cognitive radio networks with multiple antennas," *IEEE Trans. Signal Process.*, vol. 59, no. 11, pp. 5509–5522, Nov. 2011.
[9] R. Urgaonkar and M. J. Neely, "Opportunistic cooperation in cognitive femtocell networks," *IEEE J. Sel. Areas Commun.*, vol. 30, no. 3, pp. 607–616, Apr. 2012.
[10] A. Singh, M. R. Bhatnagar, and R. K. Mallik, "Cooperative spectrum sensing with an improved energy detector in cognitive radio network," in *Proc. NCC*, 2011, pp. 1–5.
[11] A. Singh, M. R. Bhatnagar, and R. K. Mallik, "Optimization of cooperative spectrum sensing with an improved energy detector over imperfect reporting channels," in *Proc. IEEE VTC— Fall*, 2011, pp. 1–5.
[12] A. Singh, M. R. Bhatnagar, and R. K. Mallik, "Cooperative spectrum sensing in multiple antenna based cognitive radio network using an improved energy detector," *IEEE Commun. Lett.*, vol. 16, no. 1, pp. 64–67, Jan. 2012.
[13] A. Singh, M. R. Bhatnagar, and R. K. Mallik, "Threshold optimization of finite sample based cognitive radio network," in *Proc. NCC*, 2012, pp. 1–5.
[14] A. Singh, M. Bhatnagar, and R. Mallik, "Threshold optimization of a finite sample-based cognitive radio network using energy detector," *EURASIP J. Wireless Commun. Netw.*, vol. 2013, no. 1, p. 165, 2013.
[15] O. Ozel and S. Ulukus, "Information-theoretic analysis of an energy harvesting communication system," in *Proc. IEEE 21st Int. Symp. PIMRC Workshops*, Sep. 2010, pp. 330–335.
[16] R. Rajesh, V. Sharma, and P. Viswanath, "Capacity of fading Gaussian channel with an energy harvesting sensor node," in *Proc. IEEE GLOBECOM*, Dec. 2011, pp. 1–6.
[17] K. Tutuncuoglu and A. Yener, "Optimum transmission policies for battery limited energy harvesting nodes," *IEEE Trans. Wireless Commun.*, vol. 11, no. 3, pp. 1180–1189, Mar. 2012.
[18] J. Yang and S. Ulukus, "Optimal packet scheduling in an energy harvesting communication system," *IEEE Trans. Commun.*, vol. 60, no. 1, pp. 220–230, Jan. 2012.
[19] C. K. Ho and R. Zhang, "Optimal energy allocation for wireless communications powered by energy harvesters," in *Proc. IEEE Int. Symp. ISIT*, Jun. 2010, pp. 2368–2372.
[20] O. Ozel, K. Tutuncuoglu, J. Yang, S. Ulukus, and A. Yener, "Transmission with energy harvesting nodes in fading wireless channels: Optimal policies," *IEEE J. Sel. Areas Commun.*, vol. 29, no. 8, pp. 1732–1743, Sep. 2011.
[21] J. Yang and S. Ulukus, "Optimal packet scheduling in a multiple access channel with rechargeable nodes," in *Proc. IEEE ICC*, Jun. 2011, pp. 1–5.
[22] L. R. Varshney, "Transporting information and energy simultaneously," in *Proc. IEEE Int. Symp. ISIT*, Jul. 2008, pp. 1612–1616.
[23] P. Grover and A. Sahai, "Shannon meets tesla: Wireless information and power transfer," in *Proc. IEEE Int. Symp. ISIT*, Jun. 2010, pp. 2363–2367.

[24] S. Luo, R. Zhang, and T. J. Lim, "Optimal save-then-transmit protocol for energy harvesting wireless transmitters," in *Proc. IEEE Int. Symp. ISIT*, Jul. 2012, pp. 955–959.
[25] L. Liu, R. Zhang, and K.-C. Chua, "Wireless information transfer with opportunistic energy harvesting," in *Proc. IEEE Int. Symp. ISIT*, Jul. 2012, pp. 950–954.
[26] R. Zhang and C. K. Ho, "Mimo broadcasting for simultaneous wireless information and power transfer," *IEEE Trans. Wireless Commun.*, vol. 12, no. 5, pp. 1989–2001, Mar. 2013.
[27] B. K. Chalise, W.-K. Ma, Y. D. Zhang, H. A. Suraweera, and M. G. Amin, "Optimum performance boundaries of ostbc based af-mimo relay system with energy harvesting receiver," *IEEE Trans. Signal Process.*, vol. 61, no. 17, pp. 4199–4213, Sep. 2013.
[28] A. Sultan, "Sensing and transmit energy optimization for an energy harvesting cognitive radio," *IEEE Wireless Commun. Lett.*, vol. 1, no. 5, pp. 500–503, Oct. 2012.
[29] S. Park *et al.*, "Optimal mode selection for cognitive radio sensor networks with rf energy harvesting," in *Proc. IEEE 23rd Int. Symp. PIMRC*, Sep. 2012, pp. 2155–2159.
[30] S. Park, H. Kim, and D. Hong, "Cognitive radio networks with energy harvesting," *IEEE Trans. Wireless Commun.*, vol. 12, no. 3, pp. 1386–1397, Mar. 2013.
[31] S. Lee, K. Huang, and R. Zhang, "Cognitive energy harvesting and transmission from a network perspective," in *Proc. IEEE ICCS*, 2012, pp. 225–229.
[32] J. N. Laneman, D. N. C. Tse, and G. W. Wornell, "Cooperative diversity in wireless networks: Efficient protocols and outage behavior," *IEEE Trans. Inf. Theory*, vol. 50, no. 12, pp. 3062–3080, Dec. 2004.
[33] T. Cover and A. E. Gamal, "Capacity theorems for the relay channel," *IEEE Trans. Inf. Theory*, vol. IT-25, no. 5, pp. 572–584, Sep. 1979.
[34] R. M. Corless, G. H. Gonnet, D. E. G. Hare, D. J. Jeffrey, and D. E. Knuth, "On the lambert w function," *Adv. Comput. Math.*, vol. 5, no. 1, pp. 329–359, 1996.
[35] S. Boyd and L. Vandenberghe, *Convex Optimization*. New York, NY, USA: Cambridge Univ. Press, 2004.
[36] M. Dohler and H. Aghvami, "On the approximation of mimo capacity," *IEEE Trans. Wireless Commun.*, vol. 4, no. 1, pp. 30–34, Jan. 2005.
[37] M. D. Springer, *The Algebra of Random Variables.* New York, NY, USA: Wiley, 1979, ser. Wiley series in probability and mathematicalstatistics.
[38] A. Papoulis, *Probability, Random Variables, Stochastic Processes*. New York, NY, USA: McGraw-Hill, 1984.
[39] R. Xie, F. R. Yu, H. Ji, and Y. Li, "Energy-efficient resource allocation for heterogeneous cognitive radio networks with femtocells," *IEEE Trans. Wireless Commun.*, vol. 11, no. 11, pp. 3910–3920, Nov. 2012.

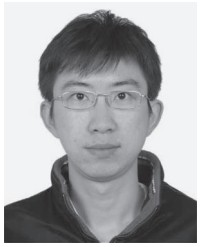

Sixing Yin (M'13) received the B.S., M.S., and Ph.D. degrees from Department of Information and Communication Engineering in Bejiing University of Posts and Telecommunications, Bejiing, China, in 2003, 2006, and 2010, respectively. He was a visiting scholar in Hong Kong University of Science and Technology, Kowloon, Hong Kong, from 2008 to 2009 and worked as a Post Doctoral Fellow in Bejiing University of Posts and Telecommunications from 2010 to 2012. He is currently an assistant professor in School of Information and Communication Engineering, Bejiing University of Posts and Telecommunications. His research interests include cognitive radio networks, spectrum measurement data analysis and energy-efficient wireless communications.

Erqing Zhang received the B.S. and M.S. degrees in 2008 and 2011, in the School of Electronic Engineering and Automation from Hangzhou Dianzi University, Hangzhou, China. She is currently pursuing the Ph.D. candidate School of Information and Communication Engineering, Beijing University of Posts and Telecommunications, Bejiing, China. Her research interests include cognitive radio networks, energy-efficient wireless communication, resource allocation and cross-layer optimization for wireless networks.

Zhaowei Qu received the M.S. degree from the Department of Computer Engineering from Kyung Hee University, Seoul, Korea, in 2002 and the B.S. and Ph.D degree from Beijing University of Posts and Telecommunications, Beijing, China, in 2002 and 2006, respectively. He is currently a reseach fellow in School of Network Technology, Bejiing University of Posts and Telecommunications. His research interests include network modeling and management and stream Control in intelligent network.

Liang Yin received the B.S. degree in the school of Electronic Engineering from Beijing University of Posts and Telecommunications, Beijing, China, in 2006. He is currently working toward the Ph.D. degree in the school of Information and Communication Engineering of Beijing University of Posts and Telecommunications. His research interests include applications associated with dynamic spectrum access, especially in analysis for spectrum measurement data and system prototype design with software-defined radios.

Shufang Li (SM'09) received the Ph.D. degree in department of electrical engineering, Tsinghua University, Beijing, China, in 1997. She is currently the Director of Ubiquitous Electromagnetic Environment Center of Education Ministry, China, and the Director of the Joint Lab of BUPT & State Radio Monitoring Center (SRMC), China. Her research interests include the theory and design technology of radio frequency circuits in wireless communication, EMI/EMC, simulation technology and optimization for radiation interfere on high-speed digital circuit, etc. She received the Young Scientists Reward sponsored by International Union of Radio Science (URSI). She has published hundreds of papers interiorly and overseas, as well as several textbooks, translation works and patents.